Wireless Energy Harvesting and Communications: Limits and Reliability

Wireless Energy Harvesting and Communications: Limits and Reliability

Jukka Rinne[1], Jari Keskinen[1], Paul R. Berger[1,2], Donald Lupo[1], and Mikko Valkama[1]

[1]Dept. of Electronics and Communications Engineering, Tampere University of Technology, Tampere, Finland
[2]The Ohio State University, Department of Electrical and Computer Engineering, 205 Dreese Laboratory, 2015 Neil Avenue, Columbus, Ohio 43210-1272, USA

Emails: jukka.rinne@tut.fi, jari.keskinen@tut.fi, paul.berger@tut.fi, donald.lupo@tut.fi, mikko.e.valkama@tut.fi

***Abstract*—Wireless energy harvesting (WEH) technique has emerged as a fascinating solution to extend the lifetime of energy-constrained wireless networks, and has been regarded as a key functional technique for almost perpetual communications. With the WEH technology, wireless devices are enabled to harvest energy from, e.g., ambient light or RF signals broadcast by ambient/dedicated wireless transmitters to support their operation and communications capabilities. The WEH technology has been expected to have even wider range of upcoming applications for, e.g., wireless sensor networks, Machine-to-Machine (M2M) communications, and the Internet of Things (IoT). In this paper, the usability and fundamental limits of solar cell harvesting based M2M communication systems are studied and presented. The theoretical performance is essentially based on the Shannon capacity theorem, combined with selected propagation loss models, assumed additional realistic link nonidealities, as well as the given energy harvesting and storage capabilities of state-of-the-art printed supercapacitor. Fundamental performance and available reliability of the communicating and harvesting functionalities are derived and analyzed, together with extensive numerical results evaluated in different practical scenarios for low power, low bandwidth, and low bitrate sensor type communication applications using organic solar cell harvester model.**

***Keywords*—Wireless energy harvesting, solar cell, M2M communications, Shannon limit, propagation loss, shadow fading, reliability, supercapacitor, perpetual communications.**

I. Introduction

Advances in technology have made it possible to implement low-cost wireless sensor network (WSN)-based automation systems [1]. Wireless sensor networks can be used for various applications including, e.g., home automation, health monitoring, factory automation, process control, real-time monitoring of machinery, monitoring environment, and real-time inventory management. In these systems, sensor nodes monitor and gather the parameters critical to automation processes and transmit the data to a user, a control center or an operator. Since sensor nodes are generally battery-powered devices, their operational lifetimes are limited. Energy harvesting techniques have a good potential to solve this constraint. It has been recently predicted, e.g. in [2], that by 2021, there will be even up to 50 billion connected devices which should all operate and integrate smoothly with the Internet while providing a vast spectrum of services in, e.g., smart cities, healthcare, smart homes, industry automation, and environmental monitoring. This trend, commonly referred to as the Internet-of-Things (IoT) or Internet-of-Everything (IoE), imposes enormous challenges and requirements on the radio connectivity in the form of Machine-to-Machine (M2M) communications, from coverage, energy-efficiency and scalability points of view [3]. Another closely related field is low-energy sensor networks and energy-harvesting, where the sensor and communication nodes are autonomously extracting or harvesting energy from their surroundings [4], [5].

Wireless systems have been evolving towards offering the users connectivity at increasingly higher data rates. While this trend is expected to continue in the fifth generation future wireless systems, there are strong indications [6], [7], [8] that also low bitrate, but high reliability communication systems will be needed in some reliability demanding applications. These are especially needed for Machine Type Communications (MTC) and/or IoT environment where, for example, critical industrial processes are controlled remotely. For this purpose, Ultra-Reliable Communication (URC) or uMTC concept is presented, providing communication service close to 100% of the time. In general, energy-autonomous M2M communications with fairly low bitrates but massive numbers of devices pose substantial demands on the component, circuit, and system designs.

One of the main technological challenges is low power consumption of the devices [9] and the methods for obtaining power or harvesting energy efficiently from different available sources, as well as storing the harvested energy [10]. In addition to the basic silicon/CMOS based circuits, also alternative organic/inorganic or printed electronics based solutions are of raising interest [11]. Organic (carbon based) electronics incorporate attractive properties of organic small molecule conductors including their electrical conductivity that can be varied by the concentrations of dopants. These potentially low cost and low carbon footprint solutions may be mechanically flexible and some have high thermal stability [12], which extend their usability in various applications.

In this paper, the feasibility and fundamental performances of energy harvesting based machine communication systems with focus on reliability, are studied and presented. In the

study, we adopt fundamental Shannon capacity laws combined with appropriate propagation loss models and assumed practical levels of nonidealities related to the radio link implementation, to extract fundamental performance limits and feasibilities for low bitrate and low energy M2M communications with given reliability. The study also incorporates solar energy harvesting considerations together with energy storage model of a realistic supercapacitor [13], [14]. We also derive expressions for the available communication distance and reliability depending on the harvested energy and storage capabilities, combined with the targeted instantaneous communication data rate and the assumed probability to transmit or receive at a given period of time. In the numerical evaluations, we specifically focus on the licence-exempt ISM band at 900 MHz (sub-1GHz) while the analysis methodology and derived expressions are valid at all other frequencies as well. The provided analysis and obtained results establish clear feasibility regions and limits on performance for energy harvesting based low-rate M2M communications.

The remainder of this paper is structured as follows. First, in Section II, the fundamental channel capacity and reliability aspects are addressed and discussed. Then, in Section III, the energy harvesting and storage issues are introduced, together with the capacitor recharging issues using harvested solar power. In Section IV, the considered path loss models are first reviewed, followed by an extensive set of numerical results. Finally, the key findings and conclusions are drawn in Section V.

II. Fundamental communication capacity and reliability

The theoretical maximum information transfer rate of any noisy channel is given by the Shannon capacity law [15]. As is very well known, this Shannon limit for communication, R, can be expressed in bits/s as

$$R = B\log_2(1 + S/N), \tag{1}$$

where B denotes the bandwidth, S refers to the received useful signal power while the noise power is denoted by N. At operational frequencies that are higher than 300 MHz, the noise is due to thermal noise [16]. In this case, the power of the noise is given by $N = kTBF$, where k, T, B, and F are the Boltzmann coefficient (1.3807×10^{-23} J/K), temperature in Kelvins, bandwidth in Hz, and noise figure (NF) in numeric form ($F = 10^{\text{NF}/10}$, where NF is in decibels), respectively. The corresponding capacity in bits/s/Hz can be then expressed as

$$C = R/B = \log_2\left(1 + \frac{S}{kTBF}\right). \tag{2}$$

To make the analysis more realistic, possible implementation losses can be taken into account in (2) by introducing an additional factor μ to model implementation losses as

$$C = \log_2\left(1 + \frac{S}{\mu kTBF}\right). \tag{3}$$

Here, $\mu \geq 1$ is related to, e.g., error correcting code strength and imperfections of receiver synchronization [17]. As an example, $\mu = 1.02$ (0.1 dB loss) if the coding system is tightly designed [18], and no other losses are present. While, e.g., $\mu = 4$ (6 dB loss) if the system is more loosely designed.

Next, to express the achievable capacity as a function of the transmit power, S_{TX}, the path loss or attenuation of the propagation channel needs to be taken into account. Thus, the received useful power S can be expressed as $S = S_{TX}/\lambda$, where λ refers to the path loss in numeric form, i.e., $\lambda = 10^{L_{\text{dB}}(d)/10}$, where $L_{\text{dB}}(d)$ refers to the pathloss in decibels at distance d. Thus, the capacity can be given by

$$C = \log_2\left(1 + \frac{S_{TX}/\lambda}{\mu kTBF}\right). \tag{4}$$

In general, when the distance, d, over which the communication may take place increases, the path loss λ increases, and hence C is decreased for given transmit power and noise related conditions. These aspects are addressed more thoroughly later in this paper, in Section IV.

As with any radio system, the propagation path loss is not static but imposes stochastic behavior in the form of shadow fading, which affects the usability or reliability of the radio link and hence communication. In order to accommodate this phenomenon, fading margin should be considered to be taken into account. To increase the reliability of communication, additional shadow fading loss should be included in the analysis. The shadowing loss is dependent on given channel scenario and is also determined by probability for which the occurrence of loss may occur. Typically, the shadow fading loss is characterized by log-normal distribution [19] with zero mean and standard deviation σ_{f} in decibels, which is normally 3 dB ... 8 dB depending on the channel scenario. For increased reliability, the considered fade margin increases correspondingly. The increase is determined by fade factor and for the required reliability in percents, $p_{\text{reliability}}(n) = 100 - 10^{-n}$, with $n = -1.6990, -1, 0, 1, 2, 3, 4$, and 5 ($p_{\text{reliability}}(n) = 50, 90, 99, 99.9, 99.99, 99.999, 99.9999, 99.99999$), the fade factors are given by

$$k_n \approx \begin{cases} 0 & \text{if } n = -1.6990 \\ 1.2816 & \text{if } n = -1 \\ 2.3263 & \text{if } n = 0 \\ 3.0902 & \text{if } n = 1 \\ 3.7190 & \text{if } n = 2 \\ 4.2649 & \text{if } n = 3 \\ 4.7534 & \text{if } n = 4 \\ 5.1993 & \text{if } n = 5 \end{cases} \tag{5}$$

By including the reliability into capacity (4), we can write capacity as

$$C = \log_2\left(1 + \frac{S_{TX}}{\lambda'\mu kTBF}\right), \tag{6}$$

where

$$\lambda' = \lambda 10^{k_n\sigma_{\text{f}}/10}, \tag{7}$$

is the path loss with shadow fading loss with a required fade factor for reliability $p_{\text{reliability}}(n)$. For example in median reliability case ($n = -1.6990$) we will have $k_n = 0$ and hence $10^{k_n\sigma_{\text{f}}/10} = 1$, whereas when e.g., $n = 3$ for 99.999 ("five nines") reliability with 3 dB standard deviation, 12.8 dB ($\approx$ 3 dB $\times$ 4.26) should be added to path loss to yield 99.999% shadow fading loss reliability requirement. In such a case this means that larger fades than the limit occurs roughly 5 minutes in a year. Moreover for ($n = 4$) 99.9999% requirement, the

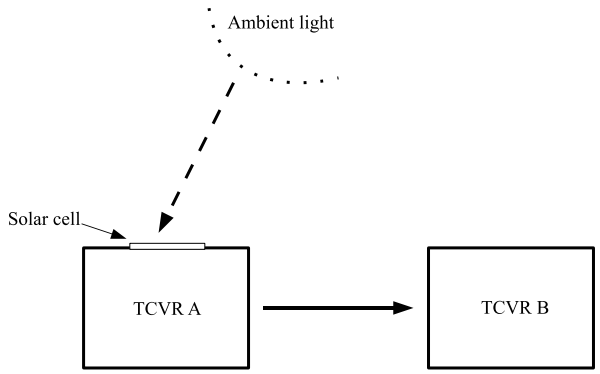

Fig. 1. Solar energy harvesting system with harvesting link (- - -) between Light source and TCVR A with solar cell and communication link (—) between TCVR A and TCVR B.

needed margin will be 14.3 dB ($\approx$ 3 dB $\times$ 4.75) for which the yearly fading limit is overlapped for 31.5 seconds. The corresponding values for ($n = 5$) 99.99999% and ($n = 6$) 99.999999% requirement are 15.6 dB and 3.2 seconds, and 16.8 dB and 0.3 seconds, correspondingly. However, from this on we will discard the latter case from our studies here due to its marginal relevance.

III. Energy harvesting, storage and power consumption aspects

A. Energy Harvesting Using Solar Cell

Energy scavenging by applying diverse methods [1], [5], [10], [20], [21], [24] like RF energy harvesting, solar energy harvesting, thermal energy harvesting allows almost perpetual use of devices and hence helps in maintaining very large systems with huge number of devices as batteries are not needed to be maintained or changed regularly. Energy can be scavenged from light using solar cell as is shown in Figure 1. The harvested energy is then used to operate transceiver for communications purposes. Communication link between transceiver (TCVR A) and remotely located transceiver (TCVR B) can be established and similarly also the TCVR B might harvest the energy with its solar cell. Typically also the possible excess harvested energy by the transceiver is stored at transceiver for later use to ensure problem-free operation in the case of sudden lighting interruption or equivalent incidence.

The amount of harvested energy depends on light illuminance and solar cell efficiency. Some typical industrial indoor lighting levels are collected to Table I. When conventional luminaires are used in lighting, the photometric maintained illuminance, E_m, in lux (lx) can be expressed as light power intensity [25], or irradiance, E in W/m^2 as

$$E = E_m/100, \tag{8}$$

and hence, e.g., 100 lx corresponds to 1 W/m^2 irradiance level and for the example lighting levels shown in Table I (200 lx...750 lx), the irradiance levels may be found to be 2 W/m^2...7.5 W/m^2 or 200 μW/cm^2...750 μW/cm^2.

TABLE I.
Lighting levels at different types of working and processing environment due to EN 12464-1 [26]

Environment	Lighting level lx
Rough assembly	200
Medium assembly	300
Fine assembly	500
Precision assembly	750

When the solar cell efficiency is, η_c, the corresponding available power intensity may be found from

$$E_s = E\eta_c. \tag{9}$$

By supposing that the solar cell efficiency is within range 3% ... 10% ($\eta_c = 0.03$ ... 0.10), the obtainable powers are 6 μW/cm^2 ... 75 μW/cm^2 (-22 dBm/cm^2 ... -11 dBm/cm^2). The given solar cell efficiency values of 3% and 10% also correspond roughly to lower and upper limit performances that are currently obtainable using organic solar cell technologies [27]. Moreover, at the moment the largest solar cell efficiency of 46.0%, is obtained by using relatively complex semiconductor multijunction cell technology.

The harvested total power, P_h, using solar cell is

$$P_h = E_s A, \tag{10}$$

where A is the surface area of solar cell. This obtained total power is the usable for transceiver operation and could be also used to maintain its energy storage.

B. Energy Storage and Power Consumption

Here, we consider supercapacitor as energy storage unit due to their good cycle life compared to secondary batteries and high energy density compared to traditional capacitors. In the case that the transceiver has receiver mode power consumption of P_{RX} and transmitter mode power consumption of P_{TX}, the total power consumption can be expressed by

$$P_{tot} = \beta_{RX} P_{RX} + \beta_{TX} P_{TX} + U I_l, \tag{11}$$

where β_{RX}, β_{TX}, U and I_l are the receive operation probability, transmit operation probability, voltage level, and leakage current of supercapacitor, correspondingly. If $P_h > P_{tot}$, there will be excessive power left over for recharging the supercapacitor, otherwise the capacitor will not be recharged and system will not be able to run perpetually. However when the charging conditions prevail, the excess power $P_e = P_h - P_{tot}$ is directed to supercapacitor with capacitance C_s, and voltage level, U, which will have energy storing capacity of $E_c = \frac{1}{2} C_s U^2$, and hence the storage supercapacitor becomes fully recharged in

$$t_c = E_c/P_e \tag{12}$$

seconds. Effectively while charging the capacitor, the transceiver operates by transmitting $3600\beta_{TX}$ seconds and receiving $3600\beta_{RX}$ in an hour. Normally transmission during receiving is not needed and we may set $\beta_{TX} = 1 - \beta_{RX}$. Furthermore, by introducing ratio of powers

$$\rho = P_{RX}/P_{TX} \tag{13}$$

between receive and transmit modes, helps us to evaluate later introduced systems more flexibly. The overhead power

consumption for the peripheral circuitry of the transmitter, $\hat{P}_{TX}$, is independent of the transmitter power consumption and diminishes the actual transmit power P_{TX}. Thus, the effective transmit power can be related to the power consumed by the transmitter as

$$S_{TX} = \alpha(P_{TX} - \hat{P}_{TX}), \tag{14}$$

where $\alpha \leq 1$ is the transmitter power efficiency. For example, α is close to 0.1 in ZigBee transceivers [21].

This concludes the description of considered scenario and more related studies with illustrative examples and evaluations will be given in Section IV.

IV. Obtained Results and Analysis

In this section, the considered channel models are briefly introduced. Later on in part B, example case is presented along with some evaluations. The focus will be in low energy, low bit rate, robust, self sufficient system, using energy harvesting.

A. Considered Pathloss Models and Use Cases

Here, IEEE 802.11ah channel models [22] are used to model a multitude of M2M communication scenarios, incorporating outdoor with macro, outdoor pico/hotzone deployments, indoor, and outdoor Device to Device (D2D) use cases. The path losses of these uses cases at distance d in meters are given by

$$L_{\text{outdoor-macro}}(d) = 8 + 37.6\log_{10}(d), \tag{15}$$

$$L_{\text{pico-hotz}}(d) = 23.3 + 36.7\log_{10}(d), \tag{16}$$

$$L_{\text{indoor}}(d) = L_{FS}(d) = 20\log_{10}(4\pi d f_c/c), \text{for } d \leq d_{BP} \tag{17}$$

$$L_{\text{indoor}}(d) = L_{FS}(d_{BP}) + 35\log_{10}(d/d_{BP}), \text{for } d > d_{BP} \tag{18}$$

where the break-point distances $d_{BP} = \{5, 5, 5, 10, 20, 30\}$ are for A...F models [22], correspondingly and

$$L_{\text{D2D}}(d) = 58.6\log_{10}(d) - 6.17, \tag{19}$$

where the attenuation is in decibels, the RF carrier frequency, f_c, is assumed to be 900 MHz, and c is the speed of light. For other center frequencies, f, a correction factor of $21\log_{10}(f/900\text{MHz})$ should be added. The given path losses are median losses and the deviation around the median to account for shadow fading loss should be modeled by adding a random Gaussian variable with zero mean and standard deviation of 8 dB for Macro deployments and 10 dB for Pico deployments. In indoor channels the standard deviation values are 2 dB when the distance is less than d_{BP}. For larger distances, the standard deviations are 3 dB for channel models A and B, and 4 dB for models C and D. Standard deviation of 5 dB is to be used for indoor models E and F. In outdoor D2D case the standard deviation is 7.5 dB.

Moreover, the Free Space Loss attenuation [23] is given by

$$L_{\text{FSL}}(d) = 20\log_{10}(d) + 20\log_{10}(f_c) - 27.55. \tag{20}$$

It should be noticed that even though the 802.11ah system itself is assumed to be deployed only at the 900 MHz (sub-1GHz) band, the above path loss models are indeed valid at other frequencies as well, as long as the proper correction factor

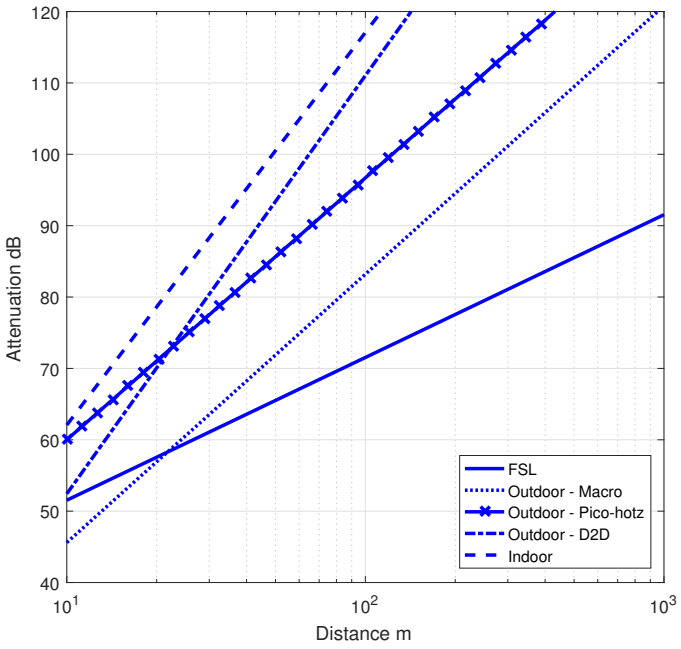

Fig. 2. (Median) Path loss for different 802.11ah channel scenarios. Here $d_{BP} = 5$ for indoor channel. Free space loss, FSL, is also shown for reference.

stated above is applied. Here in our numerical evaluations, we specifically focus on the licence-exempt ISM band at 900 MHz (sub-1GHz), due to its good suitability for low-power communications and being free from spectrum licencing related constraints. The application of interest here uses low bandwidth and low bitrate data to exchange telecontrol and telemetry status information, monitoring, e.g., the condition of machinery, temperature, humidity and similar. The principal path loss behaviors in the considered use cases versus the communication distance, d, are illustrated in Figure 2. Moreover, the capacity (6) can be evaluated for the considered channels in median path loss and, e.g., in 99.99% shadowing loss reliability case. As can be seen in Figure 3, e.g., in indoor channel when the capacity requirement is 2 bits/s/Hz, the communication distances are 58 m and 38 m, for the median and 99.99%, correspondingly. Thus, the reliability constraint diminishes the operational range by almost 30%. For 1 bit/s/Hz the corresponding distances are 71 m and 46 m.

B. Capacity and Reliability Evaluations

In this section, results of the derived capacity limits are evaluated and presented using the IEEE 802.11ah path loss model for indoor case [22]. Indoor channel A is applied with shadow fading loss. Furthermore, typical indoor lighting levels are assumed. Otherwise the parameters used in the evaluations are as follows: $B = 1$ kHz, $C = 1$ bit/s/Hz (R = 1 kbits/s), $T = 290$K, NF = 5 dB, $\alpha = 0.1$, $\rho = 1$, $\hat{P}_{TX}$ = -30 dBm, $\mu = 3.16$ (5 dB), $C_s = 0.5$ F, β_{TX}= 0.01 (β_{RX}= 0.99), $U = 1$ V, $I_l = 0.2$ μA, $A = 4$ cm^2, and $\eta_c = 0.03$ and 0.10.

First, the excess power, P_e, is evaluated with respect to illuminance for different reliability levels. The results are shown in Figure 4. For 3% solar cell efficiency case, the power levels are positive when reliabilities are smaller than 99.99 %. However, the required illumination levels are 420

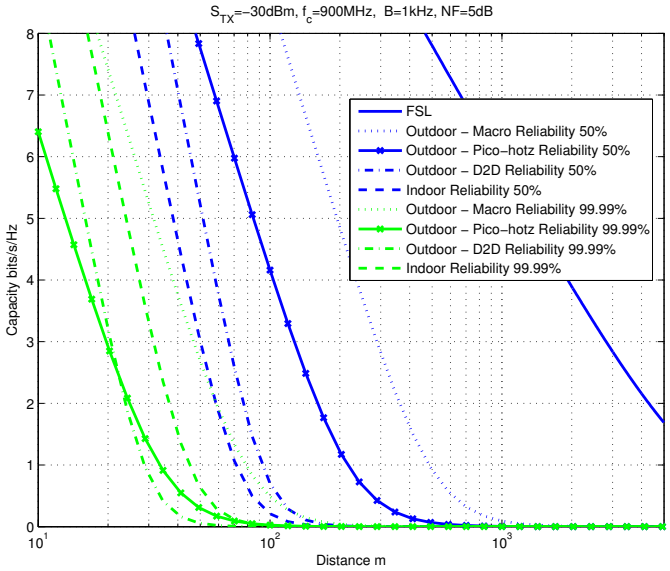

Fig. 3. Capacity wrt. distance for different 802.11ah channels at 900 MHz with reliabilities 50% and 99.99%. Here $d_{BP} = 5$ for indoor channel. Free space loss, FSL, is also shown for reference. $T = 290$K.

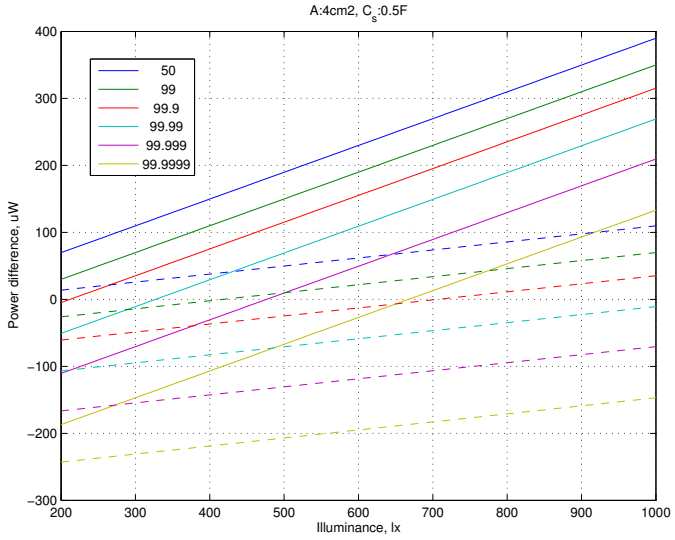

Fig. 4. Excess power, P_e, obtained during operation wrt. illuminance for different reliabilities of communication link(s) (50% ... 99.9999%) in the case of $\beta_{TX} = 0.01$, $R = 1$ kbits/s, $B = 1$ kHz, and S_{TX} = -30 dBm. Solar cell efficiency: 3% - - - and 10% —.

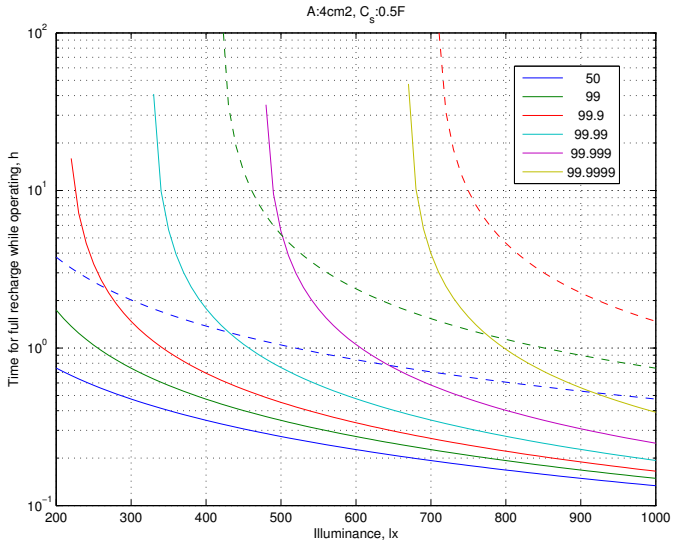

Fig. 5. Recharging time of capacitor, t_c, while operating wrt. illuminance for different reliabilities of communication link(s) (50% ... 99.9999%) for $\beta_{TX} = 0.01$, $R = 1$ kbits/s, $B = 1$ kHz, and S_{TX} = -30 dBm. Solar cell efficiency: 3% - - - and 10% —.

lx and 700 lx, for levels 99% and 99.9%, respectively. The excess power levels are negative when the reliability demand is greater than 99.9% and hence not enough power is available to fully recharge the capacitor in these cases. When the solar cell efficiency is 10 %, the excess power levels are positive as can be seen. This requires though, that the illuminance levels are 320 lx, 480 lx, and 660 lx for the most demanding reliability levels of 99.99%, 99.999%, and 99.9999%, respectively.

The required recharging times with respect to illuminance level are shown in Figure 5. With 3% efficiency when 99.9% reliability is requested, roughly 800 lx illuminance level is needed and 100 hours for the recharging of supercapacitor. When the solar cell efficiency is 10% the excess power levels are positive. This requires though, that the illuminance levels are 320 lx, 480 lx, and 660 lx for the most demanding reliability levels of 99.99%, 99.999%, and 99.9999%, respectively. The correspoding recharging times are shown in Figure 5, where drastic improvement of the performance may be noticed.

Next, we evaluate the required transmission power with respect to reliability for different distances from 10 m to 40 m (Indoor A). The results are shown in Figure 6 where it can be seen that for 40 m distance -20 dBm power level reaches 99.99999 % reliability and 90% reliability requires -32 dBm for the same path. Another interesting case is shown in Figure 7, where supercapacitor recharging time is illustrated with respect to reliability and distance for the two solar cell efficiencies. Clearly the 10% cell is better, but also 3% cell has surprisingly useful operational range. In addition, the operational time for system using supercapacitor energy is shown. Here it is supposed that only 75% of the energy can be used due to the dropping voltage level. Naturally for longer distance, i.e., larger power consumption, the functional time is limited to fractions of days for high reliability cases. For short distances ($\leq$ 20 m), operational time of one day or more may be expected.

V. Conclusion

In this paper, the limits on wireless energy-harvesting and related communications including reliability were studied and evaluated. The analysis is effectively based on Shannon theorem along with relevant path loss models and realistic implementation losses. Moreover, (organic) solar cell energy harvesting was included in the study and as a practical example a supercapacitor was adopted to store the energy scavenged. Large set of numerical results was reported to find out the feasibility regions, specifically at the licence-exempt ISM band at 900 MHz (sub-1GHz), while the presented methodology and offered results will be well usable also for evaluation of wireless energy harvesting based low-rate M2M communications

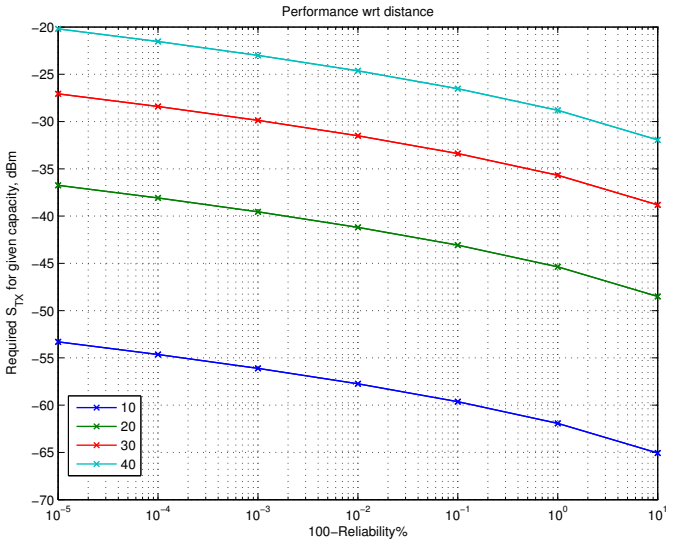

Fig. 6. Required transmission power vs. different reliabilities of communication link(s) (99.99999% ... 90%) for link distances 10 m ... 40 m. $\beta_{TX} = 0.01$, $R = 1$ kbits/s, $B = 1$ kHz.

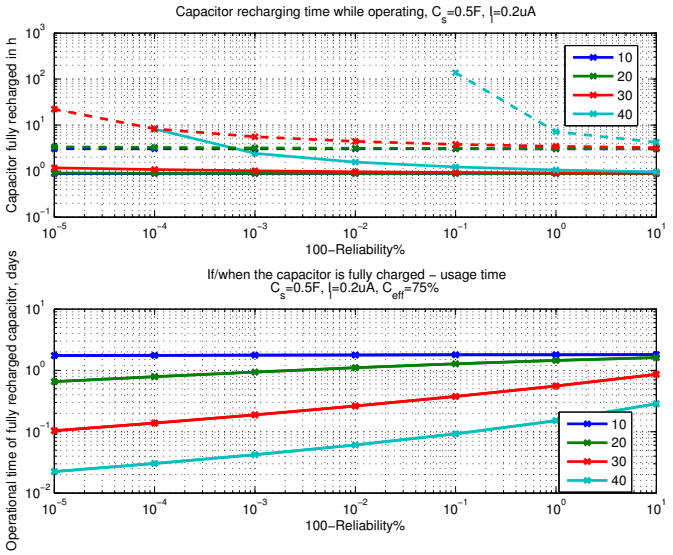

Fig. 7. Results when $\beta_{TX} = 0.01$, $R = 1$ kbits/s, and $B = 1$ kHz.
Upper figure: Capacitor recharging time vs. reliability for link distances 10 m ... 40 m. Solar cell efficiency: 3% - - - and 10% —.
Lower figure: Operational time of fully charged capacitor vs. reliability (99.99999% ... 90%) for link distances 10 m ... 40 m.

in the future IoT networks.

ACKNOWLEDGMENT

This work was financially supported by the Finnish Funding Agency for Technology and Innovation (Tekes), under the project PAUL.

REFERENCES

[1] F. K. Shaikh and S. Zeadally, "Energy harvesting in wireless sensor networks: A comprehensive review", *Renewable and Sustainable Energy Reviews* 55, pp. 1041-1054, 2016.

[2] Ericsson, Mobility report, Nov. 2015. Available [online] at http://www.ericsson.com/res/docs/2015/mobility-report/ericsson-mobility-report-nov-2015.pdf

[3] S. Andreev *et al.*, "Understanding the IoT Connectivity Landscape: A Contemporary M2M Radio Technology Roadmap," *IEEE Comm. Mag. Communications Standards Supplement*, September 2015.

[4] V. Raghunathan, C. Schurgers, P. Sung, and M. B. Srivastava, "Energy aware wireless microsensor networks," *IEEE Signal Process. Mag.*, vol. 19, no. 2, pp. 40-50, March 2002.

[5] S. Sudevalayam and P. Kulkarni, "Energy harvesting sensor nodes: Survey and implications," *IEEE Commun. Surveys Tuts.*, vol. 13, no. 3, pp. 443-461, 3rd Quart. 2011.

[6] F. Boccardi *et al.*, "Five disruptive technology directions for 5G," *IEEE Communications Magazine*, vol. 52, pp. 74-80, Feb. 2014.

[7] A. Osseiran *et al.*, "Scenarios for 5G mobile and wireless communications: the vision of the METIS project," *IEEE Communications Magazine*, vol. 52, pp. 26-35, May 2014.

[8] ITU, The Tactile Internet, ITU-T Technology Watch Report, Aug. 2014.

[9] X. Chen *et al.*, "Low power sensor design for IoT and mobile healthcare applications," *China Communications*, vol. 12, no. 5, pp. 42-54, May 2015.

[10] S. Ulukus *et al.*, "Energy Harvesting Wireless Communications: A Review of Recent Advances," *IEEE Journal on Selected Areas in Communications*, vol. 33, no. 3, pp. 360-381, March 2015.

[11] S. Lehtimaki *et al.*, "Low-cost solution processable carbon nanotube-based supercapacitors and their characterization," *Appl. Phys. A*, vol. 117, no. 3, pp. 1329-1334, Nov. 2014.

[12] G. Nisato, D. Lupo, and S. Ganz, *Organic and Printed Electronics: Fundamentals and Applications*, Pan Stanford, 2016.

[13] S. Lehtimaki *et al.*, "Performance of printable supercapacitors in an RF energy harvesting circuit," *Int. Journal of Electrical Power and Energy Systems*, vol. 58, pp. 42-46, 2014.

[14] J. Keskinen *et al.*, "Architectural Modifications for Flexible Supercapacitor Performance Optimization," *Electronic Materials Letters*, DOI: 10.1007/s13391-016-6141-y, 2016.

[15] C. E. Shannon, "A mathematical theory of communication," *ACM SIGMOBILE Mobile Computing and Communications Review*, vol. 5, no. 1, pp. 3-55, Reprinted (with corrections from Shannon 1948), 2001.

[16] Rec. ITU-R P.372-12, "Radio Noise", ITU-R Geneva, July 2015.

[17] J. G. Proakis, *Digital Communications*, 4th ed., McGraw-Hill, 2000.

[18] S. ten Brink, "A rate one-half code for approaching the Shannon limit by 0.1dB," *IEE Electronics Letters*, vol. 36, no. 15, pp. 1293-1294, July 2000.

[19] S. R. Saunders and A. Aragon-Zavala, *Antennas and Propagation for wireless Communication Systems*, 2nd ed., Wiley, 2007.

[20] M. Pinuela, P. D. Mitcheson, and S. Lucyszyn, "Ambient RF Energy Harvesting in Urban and Semi-Urban Environments," *IEEE Transactions on Microwave Theory and Techniques*, vol. 61, pp. 2715-2726, July 2013.

[21] M. T. Penella-Lopez and M. Gasulla, *Powering Autonomous Sensors: An Integral Approach with Focus on Solar and RF Energy Harvesting*, 1st ed., Springer, 2011.

[22] IEEE P802.11 Wireless LANs TGah Channel Model, (doc.: IEEE 802.11-11/0968r4), March 2015.

[23] Rec. ITU-R P.525, "Calculation of free-space attenuation," ITU-R Geneva, Aug. 2003.

[24] X. Lu *et al.*, "Wireless Networks With RF Energy Harvesting: A Contemporary Survey," *IEEE Communications Surveys & Tutorials*, vol. 17, pp. 757-789, Second Quarter 2015.

[25] S. Kitsinelis, *Light Sources*, 2nd ed., CRC Press, 2015.

[26] EN 12464-1, Light and lighting - Lighting of work places - Part 1: Indoor work places, European Committee for Standardization Brussels, 2011.

[27] NREL, Record Cell Efficiencies, Rev. 08-12-2016. Available [online] at http://www.nrel.gov/ncpv/images/efficiency_chart.jpg